Catalysis Science & Technology

Accepted Manuscript

This article can be cited before page numbers have been issued, to do this please use: J. J. Varghese, Q. T. Trinh and S. H. Mushrif, *Catal. Sci. Technol.*, 2015, DOI: 10.1039/C5CY01784J.

ROYAL SOCIETY OF CHEMISTRY

www.rsc.org/catalysis

View Article Online
DOI: 10.1039/C5CY01784J

Journal Name

ARTICLE

Insights Into the Synergistic Role of Metal-Lattice Oxygen Site Pairs in Four-Centered C-H Bond Activation of Methane: The Case of CuO

Received 00th January 20xx,
Accepted 00th January 20xx

DOI: 10.1039/x0xx00000x

www.rsc.org/

Jithin John Varghese,[†] Quang Thang Trinh,[†] and Samir H. Mushrif*

The activation of methane by transition metal/ metal oxide catalysts is pertinent for developing/optimizing processes which help to convert this abundantly available resource to value added chemicals. First principles calculations reveal that the under-coordinated lattice Cu-O pair on different CuO surfaces synergistically activates methane with barriers as low as 60.5 kJ mol^{-1} on the high energy CuO(010) surface and 76.6 kJ mol^{-1} on the most stable CuO(111) surface. The significantly low activation barrier is due to: (1) the stabilization of the transition state (TS) and the reduced strain on the dissociating methane molecule, and (2) the stabilization of the co-adsorbed products of dissociation, resulting in favorable thermodynamics. The mechanism, which is also applicable to chemisorbed oxygen containing Cu(111) surface, involves simultaneous copper addition and hydrogen abstraction by the chemisorbed/lattice oxygen via a 4-centered (CH_3-(Cu)--H-(O)) TS, stabilized by the Cu--CH_3 and O--H dipole-dipole interaction. The activation barriers for the subsequent dissociation of surface CH_3 moieties and coupling of CH_3 with CH_2 on the CuO(111) surface are both much higher than the barrier of the first C-H bond dissociation in methane. The mechanistic insights elucidated in this article could be applicable to other metal-oxygen (M-O) site pair mediated activation of methane and thus, can serve to screen potential oxide surfaces for the purpose.

1. INTRODUCTION

Methane is the most abundant hydrocarbon on the earth with large potential reserves in the form of natural gas,[1] shale gas and methane hydrates[2]. The immense potential of methane as an abundant feedstock for the upgradation to value added chemicals, fuels and high performance carbon materials remains hugely underutilized.[3] This is due to the lack of cheap and efficient materials as well as techniques to selectively and controllably activate the strong C-H bonds of methane (bond dissociation energy of ~440 kJ mol^{-1} [4]). The products of the one-step reactions for the direct transformation of methane to useful chemicals depend not only on the extent of its dehydrogenation but also on the nature and extent of functionalization/oxidation of the carbon atom.[5] Conversion of methane to commercially desirable products like ethylene requires its selective partial dehydrogenation to generate CH_3 in the gas phase or CH_x (x=2, 3) on the surface to facilitate gas phase and surface mediated coupling reactions respectively.[5] Thus, gaining a fundamental understanding of the catalytic activation process and of factors affecting it is crucial in designing catalytic reaction systems.

The relatively high activation energy barrier (150-170 kJ mol^{-1} obtained from calculations)[6-8] for the dissociation of the C-H bond of methane on copper catalysts limits its use to applications like the synthesis of graphene by chemical vapor deposition.[9,10] However, experiments on the decomposition of methane on Cu(100) surface showed that the chemisorbed oxygen on the surface can abstract hydrogen and lowers the activation energy barrier for the dissociation of methane to ~125 kJ mol^{-1} compared to ~200 kJ mol^{-1} on the clean surface.[11] Computational investigations suggest that the presence of oxygen promotes the dissociation of methane on inactive coinage metals like Cu, Ag, Au.[12,13] The suggested role of chemisorbed oxygen is to favorably alter the thermodynamic driving force for the dissociation reaction.[14] Though, the promotional effect of dissociatively chemisorbed surface oxygen on inactive metal surfaces has been revealed, detailed mechanistic insights into this are either lacking or are still a subject of debate. Moreover, chemisorbed oxygen on copper surfaces is metastable and thus doesn't constitute a stable catalytic surface as compared to its oxide counterparts.[15]

Structured oxides of certain transition metals like PdO(101), RuO_2 and IrO_2 are considered an important class of catalysts for methane activation and selective oxidation.[16,17] The activation energy barrier for the dissociation of methane involving both palladium atom and the lattice oxygen on

School of Chemical and Biomedical Engineering, Nanyang Technological University, 62 Nanyang Drive, 637459 Singapore
**Email: shmushrif@ntu.edu.sg*

† Both the authors contributed equally to this work.

Electronic Supplementary Information (ESI) available: [Complete details of the computational methodology and additional computational results supporting the concepts presented in the article]. See DOI: 10.1039/x0xx00000x

View Article Online
DOI: 10.1039/C5CY01784J

PdO(101) cluster/surface is lower than that on clean and chemisorbed oxygen covered cluster/surface.[18,19] This suggests that oxides could be better catalysts for methane C-H activation.[18,19] IrO_2(110) surface has been shown to be active not only in dissociating methane[20] but also for coupling of the dissociated CH_2 species on the surface, to form ethylene with negligible activation barriers.[21] Thus, we see that investigations of C-H bond activation on transition metal oxide surfaces focus on oxides of late 4d and 5d transition metals.

Since dissociatively chemisorbed oxygen on copper is metastable[15] and cannot bring down the activation energy barriers for the dissociation of methane to within the 100 kJ mol^{-1} range,[12] we investigated the potential of copper oxide for the same. Cupric oxide (CuO) has attracted significant attention in the recent past due to its versatility. It has been synthesized in different morphologies with a wide range of applications, including catalysis.[22] CuO has recently been demonstrated to be a very efficient and regenerative catalyst in activating the formyl C-H bonds in sugars, which is a key step in their oxidation to acids.[23] We report for the first time, the activation energy barriers and pathways for the dissociation of methane on CuO surfaces (CuO(111), CuO($\bar{1}$11) CuO(01$\bar{1}$) and CuO(010) and CuO(110)). We also provide detailed insights into the surface Cu-O site pair mediated four-centered C-H activation and dissociation which has substantially lower activation energy barriers compared to copper catalysts, with and without chemisorbed oxygen. The geometrical and electronic characteristics of the CuO surfaces and the key interactions which govern their activity towards the C-H bond dissociation are presented. In addition to activation of the first C-H bond of methane, subsequent surface reactions of the chemisorbed CH_3 species are also investigated and presented.

2. COMPUTATIONAL METHODOLOGY

The simulations were performed with the periodic plane-wave implementation of Density Functional Theory (DFT)[24,25] using the ab-initio total-energy and molecular-dynamics program VASP (Vienna ab-initio simulation program) developed at the Fakultät für Physik of the Universität Wien.[26,27] The GGA-PBE exchange correlation functional[28] within DFT and the Projector Augmented Wave (PAW)[29,30] method for the treatment of the inner core, with a plane wave cut-off energy of 450 eV were used in the electronic structure calculations. The nudged elastic band (NEB) method implemented in VASP was used to locate the transition states (TS) for the dissociation of methane on the different surfaces. The TSs were further reconfirmed with vibrational frequency calculations, where one imaginary frequency confirmed the TS. Spin polarization was turned on for all simulations involving CuO. Since DFT cannot reproduce the electronic and magnetic properties of CuO due to the strongly correlated and localized 3d electrons in copper,[31-33] the implementation of Hubbard U correction[31,34] in the form of GGA+U (LDAU in VASP) described by Dudarev et al[35] was applied to compute bulk properties and chemisorption energies on CuO surfaces. The values of U = 7.0 eV and J = 0 eV, as reported by Nolan and Elliott[32] have been used in the calculations. Since charge transfer between the surface and substrate is an important factor influencing the catalytic activity,[36,37] Bader charges[38,39] for the stable initial state configuration (IS), TS and the stable final state configuration (FS) were computed. The charge transfer mechanisms and the interactions of the reaction centers were established based on these charges.

The optimized fcc bulk lattice constant of copper was found to be 3.63 Å and was used for all subsequent calculations. Cu(111) and chemisorbed oxygen containing Cu(111) surfaces were modelled as periodic slabs with three atomic layers in 3x3 supercells with a vacuum of 10 Å above the layers, as shown in Fig. S1.a and b in the supplementary information. The first two layers were allowed to relax to account for lattice relaxation of the catalyst in the course of the reaction, while the bottom layer was fixed. A Monkhorst-Pack[40] type 4x4x1 special k-point grid was used for sampling the Brillouin zone.

CuO has a monoclinic crystal structure and the bulk lattice constant was optimized to a= 4.68 Å, b= 3.43 Å, c= 5.14 Å, β= 99.3°, which is in agreement with experimentally determined values.[41] To evaluate the potential of CuO to activate the C-H bond of methane and to understand the roles of lattice oxygen and copper in the process, we have comprehensively investigated three facets of copper oxide: CuO(111), CuO($\bar{1}$11), and CuO(110). CuO(111) has been reported to be the most stable facet among the different possible ones based on the lowest calculated surface energy and is followed by CuO($\bar{1}$11).[42] CuO(111) and CuO($\bar{1}$11) surfaces have similar surface arrangement and geometric configurations and thus would serve to reconfirm and validate the role and contribution of the metal-oxygen pair in activation. These facets of CuO chosen for investigation have been observed in experiments and can be synthesized.[23,43-45]

The surface sites on CuO(111) and CuO($\bar{1}$11) can be classified as 3-coordinated and 4-coordinated copper and oxygen atoms, with repeating arrangement of O_3-Cu_3-O_4-Cu_4, as shown in Fig. 1a and 1b. Both CuO(111) and CuO($\bar{1}$11) present adjacent pairs of under-coordinated surface lattice Cu-O site pairs which are potential active sites for methane activation and dissociation. Similar atomic arrangement with under-coordinated Cu-O pair is observed in CuO(01$\bar{1}$) and CuO(010) surfaces (supplementary information Fig. S2) and thus methane activation was investigated on these surfaces as well. CuO(110) is a higher energy surface[42] and can have two types of surface atomic arrangements: 1) Copper terminated- with repeating arrangement of Cu_2-O_4-Cu_4-O_4 where the 2-coordinated Cu atoms project out of the surface or 2) Oxygen terminated- with repeating arrangement of O_3-Cu_4-O_3, as shown in Fig. 1c and will be referred to as $CuO(110)_O$. The $Cu(110)_O$ surface is expected be more stable than the other surfaces in an oxygen rich environment.[42] On $CuO(110)_O$ surface, all oxygen atoms on the surface are 3-coordinated whereas all copper atoms on the surface are 4-coordinated. Thus, to ascertain the roles of the under-coordinated Cu-O pairs on the CuO surfaces, we investigated methane

View Article Online
DOI: 10.1039/C5CY01784J

dissociation on the $CuO(110)_O$ facet. For methane activation and dissociation, all the CuO surfaces were modelled as periodic slabs with three/four atomic layers in 3x2 supercells with 12 Å of vacuum above them (Supplementary information Fig. S1.c-g). The first two/three layers were allowed to relax while the bottom layer was fixed. The Brillouin zone was sampled with a 3x3x1 Monkhorst-Pack k-point grid in each of these cases. Further details regarding the simulation systems and supercells are given in supplementary information- section 1- Computational methodology.

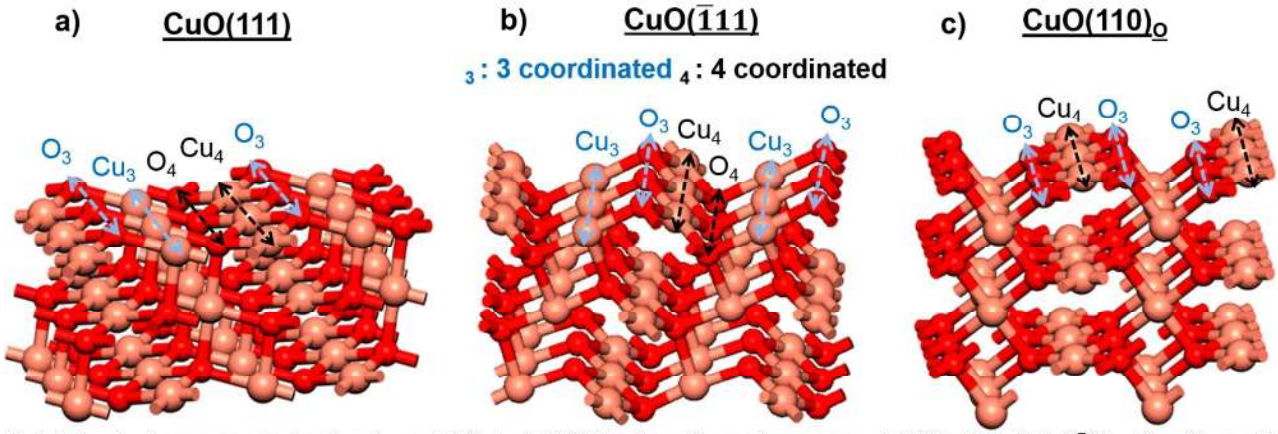

Fig. 1 Surface atomic arrangement and surface sites on CuO facets **a)** *CuO(111) surface with repeating arrangement of* O_3-Cu_3-O_4-Cu_4 **b)** *CuO(1̄11) surface with repeating* arrangement of O_3-Cu_3-O_4-Cu_4 and **c)** $CuO(110)_O$ surface with repeating arrangement of O_3–Cu_4-O_3. The peach color represents copper and the red color represents oxygen atoms.

3. RESULTS AND DISCUSSION

3.1. Activation and dissociation of methane on clean and chemisorbed oxygen containing Cu and CuO surfaces

Activation and dissociation of methane on clean Cu(111) surface is revisited for comparison with other copper and copper oxide surfaces and with the literature. Chemisorbed oxygen containing Cu(111) surface is investigated to compare and contrast the catalytic activity of the surface chemisorbed oxygen with that of lattice oxygen on CuO surfaces. Molecular oxygen (O_2) is reported to dissociatively chemisorb on Cu(111) surface with an activation energy barrier of 28 kJ mol^{-1}.[23] However, under typical catalytic conditions of high temperature and under varying oxygen pressures, copper tends to form thin oxide layers which are more stable than layers of chemisorbed oxygen (which is at best metastable[15,46]). Thus, the stable oxide surfaces of CuO with both surface copper and oxygen atoms may be more promising catalytic systems.

The activation energy barriers for the dissociation of methane in the present study are calculated with respect to the physisorbed methane on the surface. The adsorption energy of methane was studied on the clean and chemisorbed oxygen containing Cu(111) and on the CuO surfaces. The values were found to show only negligible difference (supplementary information section 2.1 and Table S1). Thus, the physisorption energy is not expected to influence the activation energy barriers significantly. The barriers calculated with respect to the physisorbed methane compare reasonably well with barriers with respect to gas phase methane (supplementary information Table S1). The reaction energy reported in this article is the difference in the energy of the system consisting of physisorbed methane on the surface, referred to as IS, and the system consisting of the fragments of dissociation in the co-adsorbed state, referred to as FS.

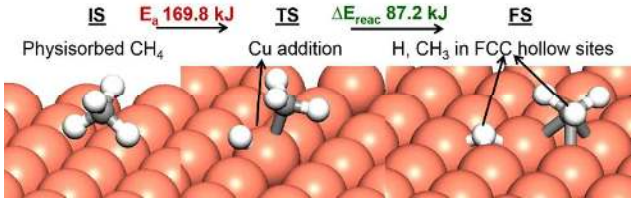

Fig. 2 Representation of the initial state (IS), transition state (TS) and final state (FS) corresponding to dissociative chemisorption of methane by oxidative addition of copper on Cu(111) surface The peach color represents copper, grey represents carbon and white represents hydrogen atoms.

The activation energy barrier for the dissociation of methane on Cu(111) surface was calculated to be 169.8 kJ mol^{-1} and compares well with the reported value of 170.8 kJ mol^{-1} in the literature.[7] The activation proceeds via a single copper atom and the products of dissociation, CH_3 and H, are both chemisorbed at the hollow sites on the copper surface, as shown in Figure 2. The reaction is highly endothermic, in agreement with literature,[7] with the reaction energy of 87.2 kJ mol^{-1}.

Distinct reaction mechanisms were investigated for the activation and dissociation of methane on the chemisorbed oxygen containing Cu(111) surface and on CuO surfaces. In the case of the chemisorbed oxygen mediated process on Cu(111), the chemisorbed oxygen at the fcc hollow site abstracts the hydrogen of methane with cooperative assistance from the surface copper atom. The result is formation of surface O-H

View Article Online
DOI: 10.1039/C5CY01784J

and CH_3 species as shown in Fig. 3a. Details of the mechanism will be discussed in section 3.2. The calculated activation energy barrier of 133.1 kJmol^{-1} is in excellent agreement with the experimentally determined values of 123 ± 27 kJ mol^{-1}.[11] The reaction energy comes down to 41.1 kJ mol^{-1} on chemisorbed oxygen containing Cu(111) compared to 87.2 kJ mol^{-1} on clean Cu(111) surface.

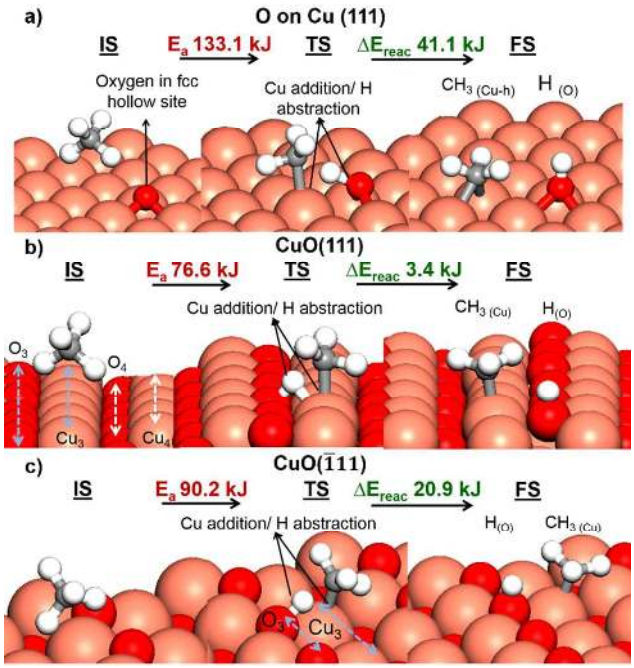

Fig. 3 Representation of the initial state (IS), transition state (TS) and final state (FS) corresponding to dissociative chemisorption of methane in a pathway involving synergistic roles of **a)** dissociatively chemisorbed surface oxygen and copper atoms on Cu(111) surface **b)** the under coordinated copper (Cu_3) and lattice oxygen (O_3) atoms on CuO(111) surface. **c)** the under coordinated copper (Cu_3) and lattice oxygen (O_3) atoms on CuO($\bar{1}$11) surface. The peach color represents copper, red represents oxygen, grey represents carbon and white represents hydrogen atoms.

On CuO(111) and CuO($\bar{1}$11) surfaces, the under-coordinated lattice oxygen (O_3) abstracts hydrogen of methane, with cooperative assistance from the under-coordinated surface copper (Cu_3) atom, forming the surface O-H and CH_3 species, as shown in Figs. 3b and 3c respectively (details of mechanism are further discussed in section 3.2). The activation energy barrier for the dissociation of methane on CuO(111) was calculated to be 76.6 kJmol^{-1}, while that on CuO($\bar{1}$11) was calculated to be 90.2 kJmol-1. To reconfirm the role of the under-coordinated Cu-O pair in the activation of methane, we also investigated other experimentally observed facets like CuO(01$\bar{1}$)[47] and CuO(010)[48] which have a similar arrangement. These facets are known to have higher surface energy compared to CuO(111) and CuO($\bar{1}$11)[42] and are thus, relatively less stable. Facets like CuO(100) and CuO(001) are terminated by either copper only or oxygen only. These surfaces would not demonstrate the synergistic mechanism that we demonstrate in the article and are thus are not investigated for methane activation. The activation energy barrier for the dissociation of methane on CuO(01$\bar{1}$) was calculated to be 95.3 kJ mol^{-1} (supplementary Fig.S3a) and that on CuO(010) was calculated to be 60.3 kJ mol^{-1} (supplementary Fig.S3b). Details regarding the dissociation on these surfaces are presented in the supplementary information section 2.2. The mechanism of activation on all these surfaces was observed to involve the under-coordinated Cu-O pair and this is responsible for the low barriers (detailed explanation in section 3.2.2). Thus, results of detailed investigation of surface phenomena associated with the activation and dissociation of methane are presented only for CuO(111), CuO($\bar{1}$11) surfaces. The low activation barriers on these CuO surfaces suggest CuO to be a much more efficient catalyst than copper. Moreover, the activation barrier on CuO(010) and CuO(111) surfaces is relatively close to that reported for more active metals like Ni, Pd and Ru, which are between 60 and 70 kJmol^{-1}.[12] The reaction energy to form stable fragments of dissociation (FS in Fig. 3b and 3c) was calculated to be 3.4 kJ mol^{-1} on CuO(111) and 20.9 kJ mol^{-1} on CuO($\bar{1}$11). These values are considerably lower than that on clean and chemisorbed oxygen containing Cu(111) surfaces.

The dissociation of methane via the aforementioned mechanism leaves the CH_3 fragment attached to the under-coordinated copper atom (Fig. 3b and 3c). With large entropy of the methyl radical (S° at 298.15 K= 194.008 J K^{-1}mol^{-1} [49]) the desorption of the surface CH_3 species is possible at high temperatures. The CH_3 fragment on the surface may also diffuse to the non-bonded under-coordinated lattice oxygen (O_3) atom. The diffusion on both CuO(111) and CuO($\bar{1}$11) surfaces was determined to proceed via a two-step mechanism as shown in Fig. 4 involving 1) diffusion from the copper atom to the adjacent copper atom which is a low barrier step and 2) hopping from the copper to the lattice oxygen atom, which is the higher barrier step. The limiting step is the hopping from copper to the bonded oxygen and the barrier was calculated to be 77.3 kJ mol^{-1} on CuO(111) surface and 57.8 kJ mol^{-1} on CuO($\bar{1}$11) surface. Thus, at typical conditions at which dissociation of methane would be carried out on these surfaces, the diffusion of CH_3 between copper atoms and from copper to lattice oxygen is highly likely. The configuration with both CH_3 and hydrogen chemisorbed on adjacent lattice oxygen (O_3) atoms on the CuO(111) and CuO($\bar{1}$11) surfaces is found to be much more stable compared to the configuration where CH_3 is on copper and hydrogen is on the lattice oxygen atom. The reaction energies with respect to these final configurations are -63.7 kJ mol^{-1} and -65.6 kJ mol^{-1} on CuO(111) and CuO($\bar{1}$11) surfaces, respectively. Thus, the formation of methyl radicals from the CH_3 fragments chemisorbed on lattice oxygen on different CuO surfaces would certainly be more challenging compared to those chemisorbed on copper atoms.

View Article Online
DOI: 10.1039/C5CY01784J

Journal Name

ARTICLE

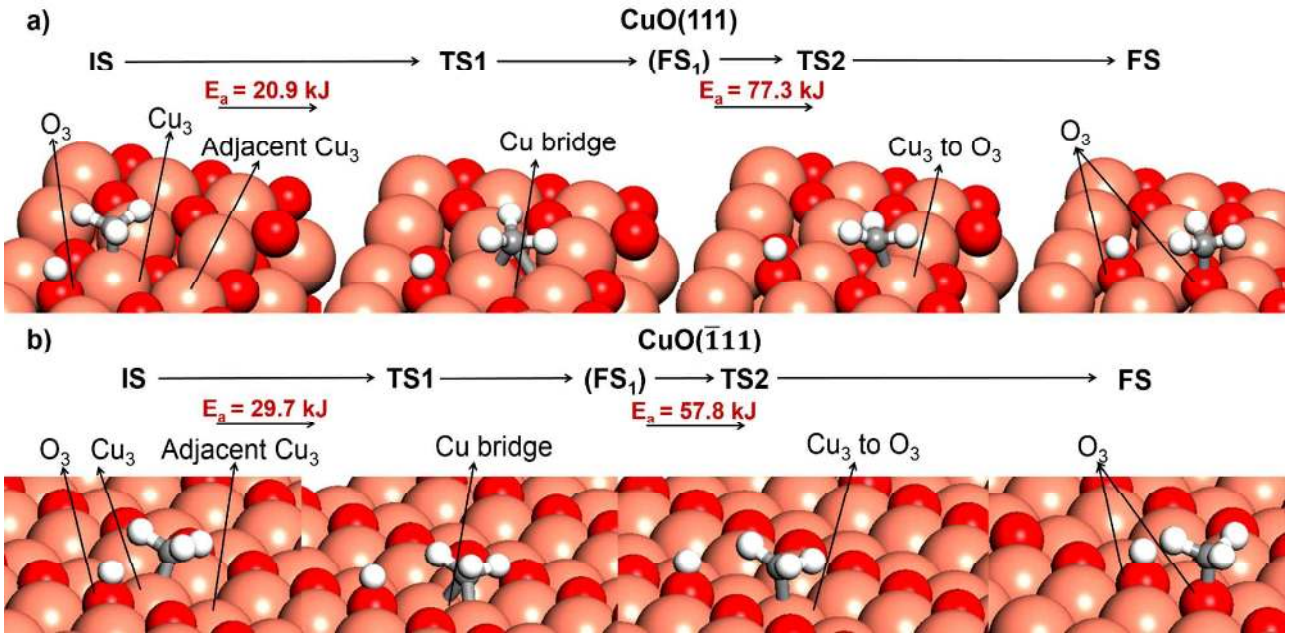

Fig. 4 Representation of the diffusion of the CH_3 group from under-coordinated copper (Cu_3) atom to the adjacent non-bonded under-coordinated lattice oxygen (O_3) atom in the two-step process on **a)** CuO(111) and **b)** CuO($\bar{1}$11). The corresponding activation energy barriers in the two stages are also shown. Color scheme same as in Figure 3.

On the chemisorbed oxygen containing Cu(111) surface, methane activation may also proceed via the involvement of the chemisorbed oxygen only, without the participation of the copper atom, as shown in Fig. 5a. The activation energy barrier in this case is 144.9 kJ mol^{-1} and is slightly higher than the case, where both the copper and chemisorbed oxygen atoms participated (Fig. 3a). Similarly, the dissociation of methane on CuO surfaces could also proceed via the involvement of the under-coordinated lattice oxygen only and without the participation of the surface copper atom. The TSs for the dissociation catalyzed by lattice oxygen only on CuO(111), CuO($\bar{1}$11) and CuO(110)O surfaces are shown in Figs. 5 b-d. The activation by this mechanism on CuO(01$\bar{1}$) and CuO(010) surfaces is presented in supplementary information Fig. S4. The activation energy barrier for dissociation of methane by this mechanism on CuO(111) surface is 130.9 kJ mol^{-1}, on CuO($\bar{1}$11) surface is 113.9 kJ mol^{-1}, on CuO(01$\bar{1}$) surface is 130.9 kJ mol^{-1}, on CuO(010) is 71.5 kJ mol^{-1} and on $CuO(110)_O$ surface is 109.1 kJ mol^{-1}. The activation energy barrier for the dissociation via this mechanism on all these surfaces is higher than when both the copper and lattice oxygen atoms are involved.

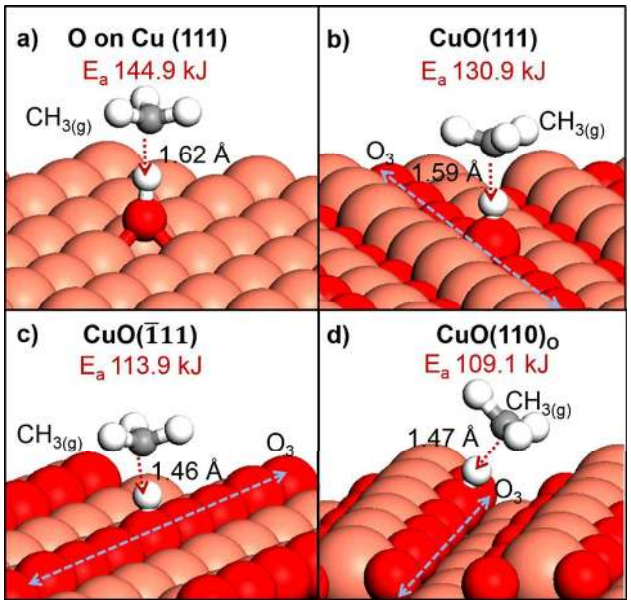

Fig. 5 Representation of the transition state (TS) corresponding to dissociation of methane in a pathway involving only hydrogen abstraction by **a)** dissociatively chemisorbed surface oxygen on Cu(111) surface **b)** the under-coordinated lattice oxygen (O_3) atom on CuO(111) surface **c)** the under-coordinated lattice oxygen (O_3)

View Article Online
DOI: 10.1039/C5CY01784J

atom on CuO($\bar{1}$11) and **d)** the under-coordinated lattice oxygen (O_3) atom on $CuO(110)_O$ surface. The activation energy barrier for dissociation on each of the surfaces is indicated and the dissociating C-H bond is indicated by the red dotted arrow along with the bond length. Color scheme same as that in Figure 3.

In each of these cases, where methane is activated by lattice oxygen alone, the dissociation results in a methyl radical, as shown in the supplementary information Figs. S5a, c, e and g. Similarly, formation of methyl radical is observed on CuO(01$\bar{1}$) and CuO(010) surfaces as well. This could be a potential pathway for the generation of methyl radicals directly in the gas phase, as the dissociating CH_3 fragment is not stabilized by any surface atom (more details in section 3.2.3). In oxidative coupling of methane on metal oxide catalysts, CH_3 radicals are known to be precursors for the formation of C_2 hydrocarbons.[50] The oxygen species on the metal oxide surfaces is believed to catalyze the dissociation of methane to form CH_3 radicals, although the homolytic or heterolytic nature of methane activation is a matter of debate.[50] Since $CuO(110)_O$ surface may not generate surface CH_3 species via the involvement of the Cu-O pair of atoms, we believe this surface may generate CH_3 species directly in the gas phase via the hydrogen abstraction pathway. However, we do not rule out the possibility of these radicals subsequently chemisorbing on the surface at low temperatures.

Since the configuration of CH_3 and hydrogen chemisorbed on adjacent lattice oxygen atoms on CuO(111) and CuO($\bar{1}$11) was found to be highly stable, we have considered the same for the chemisorption of the methyl radical on all the CuO surfaces. The adsorption of the methyl radical on the chemisorbed oxygen containing Cu(111) and the CuO surfaces along with the energetics of this chemisorption step are also shown in supplementary information Fig. S5. The reaction energies, with both CH_3 and hydrogen chemisorbed on the adjacent lattice oxygen (O_3) atoms on the CuO(111), CuO($\bar{1}$11) and $CuO(110)_O$ surfaces, are -57.5 kJ mol^{-1}, -57.7 kJ mol^{-1} and -110.3 kJ mol^{-1} respectively. The different surface configurations of CH_3 and hydrogen, observed in the different reaction pathways discussed so far, on all the Cu and CuO surfaces, are summarized along with corresponding energetics in Table 1. Thus, we see that the nature and type of active sites on copper and copper oxide surfaces determine the activation mechanism and thereby the dissociation barriers. These mechanisms are discussed in detail in section 3.2.

Table 1. Summary of the reaction pathways investigated, energetics of each of these pathways along with the configuration of the transition state (TS) and final state (FS). Two distinct reaction pathways on chemisorbed oxygen containing Cu(111), CuO(111) and CuO($\bar{1}$11) are reported. 1 and 2 on the surfaces indicate the dissociation mechanism involving the Cu-O pair and only oxygen atoms respectively. FS1 refers to the configuration with both the fragments of dissociation, CH_3 and H, co-adsorbed on the surface and FS2 refers to the configuration resulting from the diffusion of CH_3/chemisorption of CH_3 from the gas phase on the surface. (Cu) refers to top site of Cu, (Cu-h) refers to hollow site of Cu(111), (O) refers to on oxygen and (g) refers to gas phase.

Surface	TS configuration	Activation energy barrier (kJ mol^{-1})	FS1 configuration	ΔE reaction (kJ mol^{-1})	FS2 Configuration	ΔE reaction (kJ mol^{-1})
Cu(111)	$CH_{3(Cu)}$-$H_{(Cu-h)}$	169.8	$CH_{3(Cu-h)}$-$H_{(Cu-h)}$	87.2	-	-
O on Cu(111)-**1**	$CH_{3(Cu)}$-$H_{(O)}$	133.1	$CH_{3(Cu-h)}$-$H_{(O)}$	41.1	-	-
O on Cu(111)-**2**	$CH_{3(g)}$-$H_{(O)}$	144.9	-	-	$CH_{3(Cu-h)}$-$H_{(O)}$	43.0
CuO(111)-**1**	$CH_{3(Cu)}$-$H_{(O)}$	76.6	$CH_{3(Cu)}$-$H_{(O)}$	3.4	$CH_{3(O)}$-$H_{(O)}$	-63.7
CuO(111)-**2**	$CH_{3(g)}$-$H_{(O)}$	130.9	-	-	$CH_{3(O)}$-$H_{(O)}$	-57.5
CuO($\bar{1}$11)-**1**	$CH_{3(Cu)}$-$H_{(O)}$	90.2	$CH_{3(Cu)}$-$H_{(O)}$	20.9	$CH_{3(O)}$-$H_{(O)}$	-65.6
CuO($\bar{1}$11)-**2**	$CH_{3(g)}$-$H_{(O)}$	113.9	-	-	$CH_{3(O)}$-$H_{(O)}$	-57.7
$CuO(110)_O$	$CH_{3(g)}$-$H_{(O)}$	109.1	-	-	$CH_{3(O)}$-$H_{(O)}$	-110.3

3.2. Differences in methane activation mechanisms on clean Cu(111), chemisorbed O containing Cu(111), CuO(111), CuO($\bar{1}$11) and $CuO(110)_O$ surfaces

Three distinct mechanisms for the activation of methane are as follows: 1) Copper single-site three-center: Involving only copper atoms on Cu(111) surface (Fig. 6a) 2) Cu-O two-site four-center: Involving both the copper atom and chemisorbed oxygen/lattice oxygen on Cu(111)/ CuO surfaces (Fig. 6b/6c), with the exception of $CuO(110)_O$ and 3) Oxygen single-site three-center: Involving only the chemisorbed oxygen atom on Cu(111) and the lattice oxygen on the CuO surfaces (Fig. 6d). These mechanisms are discussed in detail in this section. The TS corresponding to methane activation by these three reaction pathways are depicted in Fig. 6. The active sites and reaction centers in these pathways and the relevant bond distances are also shown in the figure. The interaction between 1) methane or fragments of methane dissociation with different surfaces and 2) between the two fragments of methane dissociation are analyzed based on Bader charges on the reaction centers. The charges at the TS are shown in Fig. 6 while Table 2 reports the changes in Bader charges on the reaction centers at the TS with respect to the corresponding IS. Bader charges on all the reaction centers in the IS, TS and FS configurations along all reaction pathways are reported in supplementary information section 2.4, Table S2 and Table S3.

View Article Online
DOI: 10.1039/C5CY01784J

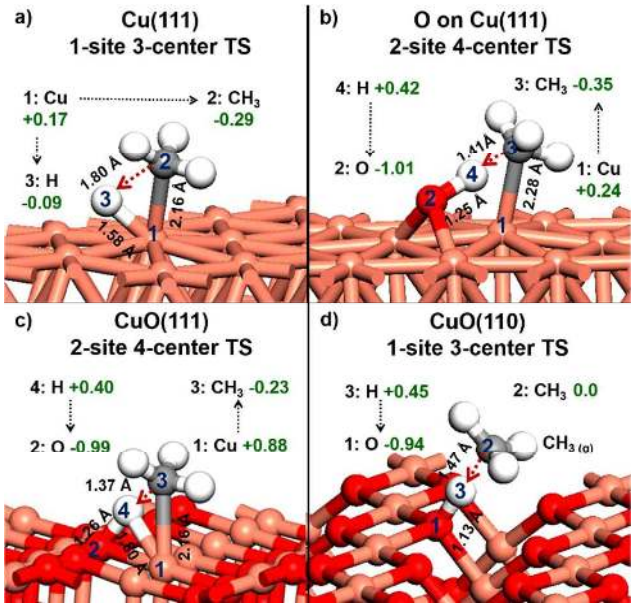

Fig. 6 Transition states (TSs) for the dissociation of methane on Cu(111) and CuO surfaces via different mechanisms **a)** copper single-site three-center mechanism on Cu(111) surface **b)** Cu-O two-site four-center mechanism on chemisorbed oxygen containing Cu(111) surface **c)** Cu-O two-site four-center mechanism on CuO(111) surface and **d)** oxygen single-site three-center mechanism on $CuO(110)_O$ surface. Bader charges on the different atoms/groups are indicated in green font. The dissociating C-H bond is indicated by the red dotted arrow, the active site and three/four reaction centers are indicated by the numbers and the charge transfer direction is indicated by the black dotted arrows. Color scheme is same as that in Figure 3.

Table 2. Changes in Bader charges on the CH_3 group, on the dissociating H of methane and on the relevant surface Cu and O atoms on different catalytic surfaces. The change is at the TS, with respect to the IS.

Surface	On CH_3 (*e*)	On dissociating H (*e*)	On chemisorbed/ lattice O (*e*)	On Cu (*e*)
Cu(111)	-0.2406	-0.1237	N.A	0.1767
O on Cu(111)	-0.2174	0.298	-0.0725	-0.0096
CuO(111)	-0.2011	0.3131	-0. 0427	-0.0208
CuO($\bar{1}$11)	-0.2031	0.3072	-0.0655	-0.0818

3.2.1. Single-site-three-centered mechanisms: Activation by copper alone

The TS on Cu(111) surface, shown in Fig. 6a, represents a single-site-three-center mechanism. Here, the surface copper atom forms the active site, and the CH_3 group, the dissociating hydrogen and the copper atom form the three reaction centers. This favors homolytic dissociation of methane and both CH_3 and hydrogen form bonds with the copper atom. During the transition from the IS to TS, the CH_3 group and the dissociating hydrogen can be seen to gain charge of 0.24 *e* and 0.12 *e*, respectively, while the copper atom loses charge of 0.18 *e* (Table 2). This, along with the close interaction of the copper atom with both the fragments suggests an oxidative addition process whereby the copper atom adds into the C-H bond of methane to form a three centered σ-complex CH_3-Cu-H (Fig. 6a). Similar three centered TS, resulting from the oxidative addition on transition metal surfaces, has been reported for methane activation and dissociation.[19,51] The charge transfer from copper to methane doesn't change the oxidation state of any copper atom on the surface completely or increase the charge on any copper atom by more than 0.2 *e* as the charge is redistributed within the atoms in the vicinity. The oxidative addition mechanism involving only the copper atom of the surface makes the interaction between the CH_3 and the hydrogen fragments at the TS repulsive, as can be seen by the positive interaction energy (supplementary information section 2.5, Table S4). The repulsive interaction between the fragments could result in the large strain on the dissociating molecule, as can be seen from the C-H bond length of 1.8 Å in the TS (Fig. 6a). Bond lengths of all four C-H bonds and the six H-C-H angles of methane in the IS and TS on different surfaces are reported in supplementary information section 2.6, Table S5. The strain on the methane molecule and the nearly negligible stabilization of the TS makes the copper single-site three-centered mechanism a very high barrier process.

3.2.2. Two-site-four-centered mechanism: Activation by Cu-O pair and dipole-dipole stabilization of TS

When the chemisorbed oxygen and the copper atom on Cu(111), and the under-coordinated Cu-O pair on CuO(111) and CuO($\bar{1}$11) surfaces participate in the dissociation, the TS features two active sites (marked 1 and 2 in Figs. 6b and 6c) and four reaction centers (marked 1-4 in Figs. 6b and 6c). The presence of chemisorbed oxygen on Cu(111) and of the lattice oxygen in CuO(111) and CuO($\bar{1}$11), facilitates the addition process described earlier by the simultaneous abstraction of the hydrogen of methane. This favors heterolytic dissociation of methane on these surfaces, as the lattice/chemisorbed oxygen polarizes the C-H bond, while copper adds across it. The concepts and principles discussed in this section are also applicable to the activation on CuO(01$\bar{1}$) and CuO(010) surfaces. Metal oxides are known to be bifunctional catalysts with acidic and basic sites that can induce heterolytic dissociation of molecules.[52] On chemisorbed oxygen containing Cu(111), the CH_3 group at the TS is observed to gain charge of 0.22 *e* in the course of the dissociation while the hydrogen atom loses charge of 0.3 *e* (Table 2). However, there is negligible change in the charge on the copper atom and on the chemisorbed oxygen atom. Similarly, on the CuO(111) and CuO($\bar{1}$11) surfaces, the CH_3 group is observed to gain charge of 0.2 *e* and the hydrogen atom loses charge of 0.31 *e* (Table 2). The change in charges on the copper and lattice oxygen atoms on the surface are negligible. The negligible change in charges on the copper and oxygen atoms of chemisorbed oxygen containing Cu(111), CuO(111) and CuO($\bar{1}$11) surfaces, when the charges on the CH_3 group and the hydrogen atom change, suggests a cyclic concerted charge transfer involving four reaction centers (Cu→CH_3---H→ O→ Cu). The charge lost by the copper atom in forming the Cu-CH_3 is recovered when the chemisorbed oxygen/lattice oxygen redistributes it among the

View Article Online
DOI: 10.1039/C5CY01784J

connected copper atoms by accepting charge from the dissociating hydrogen (charges on all reaction centers are reported in supplementary information section 2.4, Table S2). Such four-centered TS and concerted charge transfer interaction has been reported for chemisorbed oxygen and platinum atom mediated activation on Pt clusters[51] and for the lattice oxygen and palladium atom mediated activation on Pd(101) clusters.[19] Copper addition to the C-H bond and concerted hydrogen abstraction by the chemisorbed/lattice oxygen is reminiscent of the 'σ bond metathesis'- like pathway reported on chemisorbed oxygen containing Pt clusters[51] and PdO clusters.[19] This four centered TS is much more stable than the three centered TS described earlier, as the four reaction centers carry complementary charges enabling dipole-dipole like interactions ($(Cu^{\delta+}\text{-}CH_3^{\delta-})\text{---}(O^{\delta-}\text{-}H^{\delta+})$). Dipole-dipole interactions have been reported to stabilize transition states and bring about favorable changes in the activation energy barriers.[53] The TS in the activation of methane involving only copper addition on Cu(111) is not stabilized by such interactions and thus has a much higher activation energy barrier.

The interaction between the CH_3 and hydrogen fragments at the TS changes from repulsive on clean Cu(111) to attractive on the chemisorbed oxygen containing Cu(111), CuO(111) and CuO($\bar{1}11$), when both the copper and lattice oxygen atoms participate in the activation. This is evident from the negative interaction energy between these fragments as reported in supplementary information Table S4. The attractive interaction may also explain the much shorter dissociating C-H bond on these surfaces (1.41 Å on chemisorbed oxygen containing Cu(111), 1.37 Å on CuO(111) and 1.39Å on CuO($\bar{1}11$)) compared to 1.8 Å on clean Cu(111) surface (geometry of methane in the IS and TS on different Cu and CuO surfaces is provided in supplementary information section 2.6, Table S5). Shorter dissociating C-H bonds imply lesser strain on the dissociating methane molecule. Thus, the dipole-dipole interaction stabilizes the TS by virtue of the substrate-adsorbate charge transfer interaction and by enabling favorable interaction between the dissociating fragments, thereby lowering the strain on the dissociating molecule. The latter two factors are key to lowering the activation energy barriers for the dissociation of molecules as per the activation strain model proposed by Bickelhaupt and co-workers.[54,55]

In addition to the stabilization of the TS, the participation of both, copper and oxygen atoms in the activation and dissociation also lends stability to the co-adsorbed products of the dissociation. The reaction energy for the dissociation of methane decreases from 87.2 kJ mol^{-1} on Cu(111) to 41.1 kJ mol^{-1} when both the copper and oxygen atoms participate in the activation on chemisorbed oxygen containing Cu(111). The significant decrease in the reaction energy due to the presence of the chemisorbed oxygen on the surface brings about a corresponding reduction in the activation energy barriers. This is in agreement with the proposition by Nørskov and co-workers[14] that for C-H activation, the role of chemisorbed oxygen on metals is to alter the thermodynamics of the reaction and thereby reaction barriers. The reaction energy is further lowered on CuO(111) and CuO($\bar{1}11$) surfaces to 3.4 kJ mol^{-1} and 20.9 kJ mol^{-1}, respectively, when the Cu-O pair are involved in the activation. Figure 7 shows the nearly linear correlation of the activation energy barriers and the reaction energies on these surfaces (more details on the linear correlation of activation energy barrier and reaction energy is presented in supplementary information section 2.7). Figure 7 suggests that the more favorable reaction energy on CuO(111) and CuO($\bar{1}11$) surfaces compared to chemisorbed oxygen containing Cu(111) and clean Cu(111) could be one of the reasons for the much lower activation energy barriers on oxide surfaces (Table 1). Between CuO(111) and CuO($\bar{1}11$) surfaces, the reaction energy is more favorable on CuO(111) and thus the barrier is lower on it. It has been shown that for metal oxides, the dissociative chemisorption energy becomes a descriptor for the activation energy barrier only if the geometry of the TS resembles to that of the FS.[56] The TS on the clean Cu(111), chemisorbed oxygen containing Cu(111), CuO(111) and CuO($\bar{1}11$) surfaces is 'late', resembling the FS, with almost dissociated C-H bonds/nearly formed O-H species (Fig. 2 and Fig. 3). This is in agreement with literature showing the TS for C-H bond activation on metals and chemisorbed oxygen containing metals to be 'late'.[14]

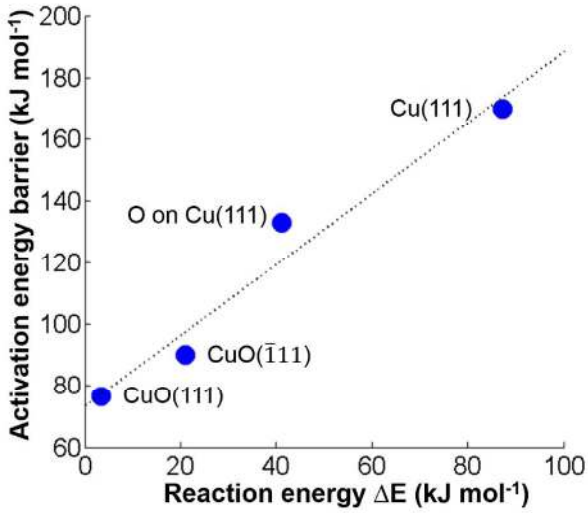

Fig. 7 Plot of the activation energy barrier for the dissociation of methane on copper and copper oxide surfaces against the corresponding reaction energy, suggesting a nearly linear correlation of the two quantities. All the reactions considered are endothermic and thus the reaction energies are positive.

Additionally, there exists a nearly linear correlation between the energy of the TS and the energy of the FS, with the slope close to one, reconfirming the 'late' TS on these surfaces (supplementary information section 2.7, Fig. S7). This possibly explains the Brønsted-Evans-Polanyi (BEP) like relationship (Fig. 7), typically observed in transition metal catalyzed dissociation reactions,[57,58] to exist for the CuO surfaces as well. Thus, for the oxygen containing surfaces, with both the copper and oxygen atoms participating in the activation of methane, the activation energy barriers are

View Article Online
DOI: 10.1039/C5CY01784J

influenced by the stabilization of the TS as well as that of the co-adsorbed products.

3.2.3. Single-site-three-centered mechanisms: Activation by oxygen alone

The TS for methane dissociation by the chemisorbed oxygen on Cu(111) or by the under- coordinated lattice oxygen (O_3) in CuO(111), CuO($\bar{1}11$) and CuO(110)$_O$ only, shown in Fig. 5 and Fig. 6d, suggests a single-site three-center pathway. The chemisorbed oxygen or under-coordinated lattice oxygen (O_3) atom is the active site instead of the copper atom. The principles discussed here are also applicable to dissociation of methane involving only lattice oxygen on CuO(01$\bar{1}$) and CuO(010) surfaces. The dissociating CH_3 fragment is not stabilized by any surface atom and thus forms a radical in this homolytic dissociation pathway. The formation of the methyl radical can be confirmed by near planar sp2 structure of the species in the gas phase FS (supplementary information Figs. S5a, c, e, g) and the near neutral charge on the group (less than 0.05 *e*) on all the surfaces, as seen from the Table S3 of the supplementary information. Such hydrogen abstraction mechanism with relatively high barriers via the formation of a free methyl radical has been reported on oxygen saturated Pt[51] and Pd[19] clusters. Unlike the copper atom, the lattice oxygen (O_3) atoms adjacent to the one abstracting the hydrogen are unable to interact with the CH_3 group during the dissociation. On CuO(110)$_O$, the surface Cu atoms are 4-coordinate and thus are unable to participate in the 'σ bond metathesis' like two-site four-centered mechanism observed on the other CuO surfaces. The absence of synergy in this oxygen only single-site three-center pathway results in the activation energy barrier for the dissociation being much higher than the pathway involving the Cu-O pair of atoms (Table1). The activation barrier follows the trend: chemisorbed oxygen containing Cu(111) > CuO(111) ~ CuO(01$\bar{1}$) > CuO($\bar{1}$11) > CuO(110)$_O$ > CuO(010). Thus, the lattice oxygen on the CuO surfaces are more efficient in abstracting hydrogen of methane compared to chemisorbed oxygen on Cu(111). Moreover, the activation by lattice oxygen alone on the CuO surfaces have barriers equivalent to or lower than the mechanism involving the Cu-O pair on chemisorbed oxygen containing Cu(111). This decisively shows that CuO surfaces are catalytically more active than clean and chemisorbed oxygen containing copper, irrespective of the nature of the activation mechanism.

3.3. Nature/ characteristics of the surface sites and their implications for activation energy barriers and reaction energies

The charges on surface atoms and the bonding of metal and oxygen in chemisorbed oxygen containing Cu(111) and CuO surfaces have implications on the stabilization of the TS and the FS. Thus, these factors may not only dictate the reaction pathways on these surfaces but also influence the energetics. Dissociatively chemisorbed oxygen on Cu(111) is coordinately bonded to the surface and the surface essentially retains its metallic character. Bader charges on the surface copper atoms (except those connected to the O atom) are close to 0 suggesting the metallic nature of the surface (supplementary information section 2.4, Table S2). As with most late transition metal oxides of the reducible kind[59] the bonding in CuO is known to be a mix of covalent and ionic[60]. Bader charges (supplementary information section 2.4, Table S2 and S3) on the surface copper and oxygen atoms on the CuO surfaces suggest a fair degree of ionic character. The charge on the copper atoms coordinated with the chemisorbed oxygen in Cu(111) surface (0.24 *e* and less), is much lower compared to 0.86 *e* and 0.79 *e* on the under-coordinated copper atoms in CuO(111) and CuO($\bar{1}$11) surfaces, respectively. The charge on the oxygen atoms in these surfaces is nearly similar with -0.93 *e* on the chemisorbed oxygen on Cu(111), -0.95 *e* and -0.89 *e* on the under-coordinated surface lattice oxygen atoms of CuO(111) and CuO($\bar{1}$11), respectively. The strong dipole-dipole interactions that stabilize the TS on CuO(111) and CuO($\bar{1}$11) surfaces are a result of these complementary charges on the Cu-O site pairs and the resulting charge transfer described in section 3.2.2. The complementary charges on the four reaction centers in the TS and the FS, as shown in Fig. 6 and in the supplementary information Table S2, have higher magnitude on CuO(111) and CuO($\bar{1}$11) surfaces, compared to chemisorbed oxygen containing Cu(111). Thus, the stabilization of the TS and the FS is expected to be greater on CuO(111) and CuO($\bar{1}$11) surfaces than on chemisorbed oxygen containing Cu(111). This may be the reason for the significantly lower activation energy barriers for the dissociation of methane on CuO(111) and CuO($\bar{1}$11) than on chemisorbed oxygen containing Cu(111), in the Cu-O two-site four-center mechanism.

Table 3. Binding energies of the chemisorbed surface oxygen on Cu(111) and of the under-coordinated surface lattice oxygen atoms (O_3) on different CuO facets. Also reported are the chemisorption energies of hydrogen and CH_3 on the chemisorbed surface oxygen on Cu(111)/ under-coordinated surface lattice oxygen (O_3) on CuO surfaces, and adsorption energies of CH_3 on the copper atoms adjacent to chemisorbed oxygen on Cu(111)/ under-coordinated copper atoms (Cu_3) on the CuO surfaces. All the reported values are calculated as reaction energies and thus larger positive values indicate lower binding strength. Refer supplementary information for details about the calculation methodology.

Surface	Chemisorbed/ lattice oxygen (O_3) binding energy (kJmol^{-1})	H chemisorption energy on chemisorbed O/ O_3 (kJmol^{-1})	CH_3 chemisorption energy on chemisorbed O/ O_3 (kJmol^{-1})	CH_3 chemisorption energy on Cu/ Cu_3 (kJmol^{-1})
O on Cu(111)	84.8	-76.8	45.9	113.2
CuO(111)	26.6	-91.3	41.2	133.3
CuO($\bar{1}$11)	51.7	-108.9	29.4	137.9
CuO(110)O	147.14	-188.9	-42.8	N.A.

The strength of Cu-O bonding in different CuO surfaces possibly influences the activation barriers for the dissociation of methane in the oxygen only single-site three-center

View Article Online
DOI: 10.1039/C5CY01784J

pathway. It may also determine the chemisorption energies of the fragments of dissociation on these surfaces and thereby the reaction energies. From Table 3, it can be seen that the binding energy of the under-coordinated lattice (O_3) atom in different surfaces follow the order CuO(111) > CuO($\bar{1}$11) >CuO(110)$_O$. The binding energy of the lattice oxygen on the CuO surfaces is interpreted as the energy to insert an oxygen atom into an oxygen vacancy on the surface (details of the calculation are given in supplementary information section 2.8). This gives an estimate of the Cu-O bond strength on the different CuO surfaces. The weaker the interaction of oxygen with copper, the stronger will be its interaction with adsorbates and its ability to abstract hydrogen. It is observed from Table 1 that the activation energy barriers for the dissociation of methane by hydrogen abstraction alone by 3-coordinated lattice oxygen on the three CuO surfaces follow the trend of CuO(110)$_O$ < CuO($\bar{1}$11) < CuO(111). The weakly bound lattice oxygen on CuO(110)$_O$ abstracts hydrogen from methane much better compared to lattice oxygen atoms on CuO($\bar{1}$11) and CuO(111) surfaces. Table 3 also shows that the chemisorption energies of hydrogen and CH_3 (each individually) to the lattice oxygen (O_3) atom on these surfaces follows the trend of CuO(110)$_O$ > CuO($\bar{1}$11) > CuO(111). Details of calculation methodology are given in supplementary information section 2.8. The reaction energy, with both CH_3 and hydrogen are co-adsorbed on the lattice oxygen atoms on CuO(110)$_O$, has a large negative value (exothermic) of -110.3 kJ mol^{-1}. The corresponding values are -57.7 kJ mol^{-1} on CuO($\bar{1}$11) and -57.5 kJ mol^{-1} on CuO(111) surfaces (Table 1). In contrast, the reaction energies were positive when the CH_3 and the hydrogen co-adsorbed on the Cu-O site pairs on these surfaces. The strong binding of hydrogen and CH_3 on the CuO(110)$_O$ surface suggests that subsequent surface reactions and desorption of the fragments from the surface would be more difficult than on CuO(111) and CuO($\bar{1}$11). For catalytic reactions, a balance between the activation efficacies of the catalyst and product recoverability is desired. The former may be determined by the strength of interaction of the reactant or the TS with the surface and the latter is determined by the chemisorption strength of the products. CuO(111) surface can be seen to exhibit the best balance among the surfaces investigated here. The CuO(110)$_O$ surface, on the other hand, may generate free methyl radicals by the oxygen only single-site three-center mechanism at high temperatures.

For chemisorbed oxygen on different metal surfaces, the strength of the interaction of oxygen with the surface has been shown to be a key factor determining its efficacy in promoting methane activation.[12,13] During activation of methane, the chemisorbed oxygen on Cu(111) can be seen to be pushed from its fcc hollow site towards the bridge site of the copper atoms opposite the CH_3 group (Figure 6b). This is to accommodate the CH_3 at the copper site. The repulsion between the chemisorbed oxygen and CH_3 also elongates the Cu-CH_3 bond by 0.12 Å compared to the same on Cu(111). The dislodging of the chemisorbed oxygen from the Cu(111) fcc hollow site to the bridge site at the TS (Fig,6b), is possible due to its relatively weak binding on the Cu(111) surface. The weak binding can be gauged by the binding energy of 84.8 kJ mol^{-1}. This explains why the promotional effect of chemisorbed oxygen is observed only on inactive coinage metals where the binding of chemisorbed oxygen on the surface is weak, as shown by Xing *et al*.[12,13] If the chemisorbed oxygen is strongly bound, it cannot be displaced from its hollow site position and thus weakens the M-CH_3 (where M is a metal) interaction which is essential for the activation process.

3.4. Subsequent reactions of chemisorbed CH_3 on CuO(111)

CuO(111) surface has shown the best balance between the activation efficacy for methane dissociation and the chemisorption strength of the fragments of dissociation among the CuO surfaces investigated here. Additionally, it is the most stable surface which can be experimentally synthesized.[23] Thus, subsequent reactions of chemisorbed CH_3 species are investigated on it. Chemisorbed CH_3 on the CuO(111) surface may undergo further dissociation and surface reactions. The barrier for diffusion of CH_3 between the under-coordinated (Cu_3) atoms on CuO(111) was calculated to be 21 kJmol^{-1} (Fig. 4) and thus CH_3 migration from one copper atom to a free adjacent copper atom is highly likely. Thus, the dissociation of chemisorbed CH_3 is evaluated without the dissociated and co-adsorbed hydrogen at the adjacent under-coordinated lattice oxygen atom.

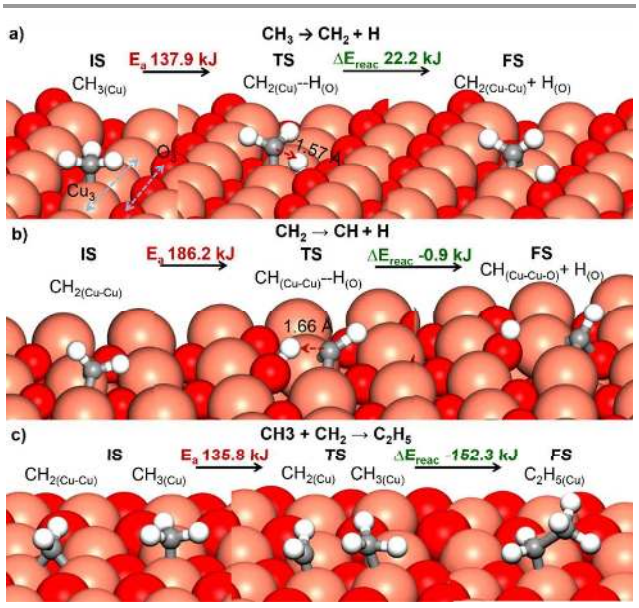

Fig. 8 Representation of the initial state **(**IS), transition state (TS) and final state (FS) corresponding to **a)** the dissociation of chemisorbed CH_3 on CuO(111) surface **b)** the dissociation of chemisorbed CH_2 on CuO(111) surface. The dissociating C-H bond at the TS is depicted by the red dotted arrow. **c)** The coupling of CH_3 and CH_2 fragments on the CuO(111) surface to form C_2H_5 which is bound to the surface. The activation energy barrier and the reaction energy in each of the cases are also shown. Color scheme is same as that in Figure 3.

The activation energy barrier for the dissociation scheme of CH_3, as depicted in Fig. 8a, is calculated to be 137.9 kJ mol^{-1} and is much higher than that of the dissociation of methane.

View Article Online
DOI: 10.1039/C5CY01784J

The barrier is comparable to that of the dissociation of CH_3 on Cu(111) reported in literature.[6] The dissociation of CH_3 necessitates reorganization of the CuO lattice to enable CH_2 to form bonds with two adjacent copper atoms. This allows it to maintain the sp^3 nature of the C center, as shown in Fig. 8a. The overall lattice reorganization and geometric constraint lead to a longer dissociating C-H bond of 1.57 Å at the TS. The dissociation of CH_2, bound to two copper atoms, has an even higher activation energy barrier of 186.2 kJ mol^{-1} and the reaction scheme is shown in Fig. 8b. The barrier is nearly double that of the corresponding step on clean Cu(111) surface which is reported to be ~90 kJ mol^{-1} [6]. The resulting CH species is bound to two copper atoms and an adjacent lattice oxygen atom in a distorted tetrahedron. The significant lattice reorganization in this step could be a reason for the large activation energy barrier. Subsequent dissociation to C is not investigated due to the large barriers for the formation of surface CH species.

The CH_3 species on CuO(111) surface may undergo surface mediated coupling with CH_2 to form C_2H_5 which is bound to the surface, as shown in Fig. 8c. The activation energy barrier for this coupling pathway is 135.8 kJ mol^{-1}, which is nearly the same as that for the dissociation of CH_3 to CH_2. Thus the CH_2 formed on the surface may readily couple with available CH_3 on the surface to form C_2H_5, as the reaction is energetically favorable as well. C_2H_5 has been suggested to be an important intermediate in the formation of large hydrocarbons from methane on copper surface[61] and clusters[62]. Surface reactions of CH_3 chemisorbed on the lattice oxygen may generate oxygen containing species, although an exhaustive investigation of the different pathways is beyond the scope of this article.

4. SUMMARY AND PERSPECTIVE

This article reports facile C-H bond activation of methane on different facets of copper oxide and contrasts the two potential mechanisms for the reaction on these surfaces. When mediated by a pair of adjacent under-coordinated Cu-O surface sites, the strong C-H bonds of methane can be cleaved with an activation energy barrier of 76.6 kJ mol^{-1} on the stable CuO(111) surface and 90.2 kJmol^{-1} on CuO($\bar{1}$11) surface. High energy CuO surfaces may dissociate methane with lower activation barriers via the same mechanism, as seen from the example of CuO(010) surface where the barrier is only 60.5 kJ mol^{-1}. The heterolytic C-H bond dissociation on the under-coordinated Cu-O site pairs of CuO surfaces proceeds via copper addition to the C-H bond of methane and the concerted hydrogen abstraction by the lattice oxygen. The CH_3 group, the dissociating hydrogen, and copper and oxygen atoms form a 4-centered TS which is stabilized by the dipole-dipole interaction (CH_3—Cu and H—O). This is facilitated by a concerted cyclic charge transfer process involving the four centers (Cu→CH_3---H→ O→ Cu). These interactions also reduce the strain on the dissociating methane molecule and in turn lower the activation energy barriers. Similarly, the Cu-O pair on chemisorbed oxygen containing Cu(111) surface activates methane via the same two-site four-centered mechanism, but with higher activation energy barrier of 133.1 kJ mol^{-1}. The lesser extent of stabilization of both, the transition state and the final state by dipole-dipole interactions, compared to that on CuO(111) and CuO($\bar{1}$11) surfaces is the reason for the higher barrier. Thus, CuO is found to be a much better catalyst for methane activation, compared to copper.

In contrast, the dissociation of methane on clean Cu(111) surface proceeds by a single-site three-centered mechanism involving only copper atom addition to methane. The homolytic dissociation of methane on Cu(111), makes it a high barrier process, with the activation energy barrier of 169.8 kJ mol^{-1}. On chemisorbed oxygen containing Cu(111) and the CuO surfaces, methane activation may also proceed by the involvement of only the oxygen species as active sites in a hydrogen abstraction mechanism: another single-site three-centered process. This pathway also has higher activation energy barriers compared to the concerted mechanism involving the Cu-O pair and additionally it leads to the formation of methyl radicals. Due to the absence of under-coordinated copper atoms on its surface, the hydrogen abstraction mechanism may be the only pathway for methane activation on $CuO(110)_O$ surface, unlike the other CuO surfaces. The absence of the stabilization of the TS in these two single active site (either Cu or O) and three-centered mechanisms is the prime reason for the considerably higher barriers for methane activation, compared to the two-site four-centered concerted copper addition and hydrogen abstraction mechanism. On CuO surfaces, the surface Cu-O bond strength determines the ability of the lattice oxygen to abstract and chemisorb hydrogen. Thus, among the surfaces with 3-coordinated surface lattice oxygen, $CuO(110)_O$ surface with low Cu-O binding strength, exhibits the lowest activation energy barrier for methane activation by the hydrogen abstraction mechanism (oxygen single-site three-center mechanism).

The successive dissociation of chemisorbed CH_3 on CuO(111) to CH_2 and further to CH have activation energy barriers of 137.9 kJ mol^{-1} and 186.2 kJ mol^{-1}, respectively. The barrier is progressively increasing at each dehydrogenation stage and both values are much higher than that of the first C-H bond dissociation on CuO(111). This is in contrast to dissociation on Cu(111) surface where the barrier for the first dissociation is high and progressively decreases until the last dehydrogenation step to form carbon, which has the highest barriers among the four steps.[7] The large difference in activation barriers for the first C-H dissociation of methane on CuO(111) and the subsequent dehydrogenation steps can be exploited to selectively generate CH_3 species. The reaction conditions may be tuned such that the methane dissociation by both the mechanisms described in the article generates CH_3 species; either chemisorbed on the surface or in the gas phase. At such conditions, the successive surface dehydrogenation of CH_3 species and surface coupling reactions to form larger hydrocarbons may not be significant. CH_x species (x= 1 to 3) on the surface of Cu(111) is known to be responsible for growth

View Article Online
DOI: 10.1039/C5CY01784J

of graphene[7,63] which might not happen on CuO surfaces. The free methyl radicals generated by the 'oxygen only single-site mechanism' would serve as precursors for coupling reactions. In coupling reactions involving methane to produce ethylene and aromatics, the role of the catalytic surface is typically limited to generating free methyl radicals while the coupling to ethane, subsequent thermal dehydrogenation to ethylene and formation of aromatics are all gas phase reactions.[50,64,65] Surfaces like $CuO(110)_O$ may also selectively generate methyl radicals in the gas phase, via the 'oxygen only single-site mechanism' mechanism. Single-site copper-oxo complexes in zeolites have been recently shown to be highly reactive in the homolytic dissociation of methane and its conversion to oxygenates like methanol.[66] Thus, the CH_3 species chemisorbed on the CuO surfaces may undergo surface reactions and rearrangements with the lattice oxygen to generate oxygen containing species as well.

We believe that the mechanistic insights from the two-site four-center C-H activation by the under-coordinated Cu-O pair described here can be extended to all reducible transition metal oxides exposing under-coordinated surface metal and oxygen site pairs. Thus, we hope that this article provides a guideline for screening multifunctional metal oxide based catalytic surfaces/facets for selective C-H bond activation and conversion to other value added chemicals.

Acknowledgements

This work is financially supported by Nanyang Technological University, Singapore. We thank the anonymous reviewers for their comments and suggestions, which helped us improve the manuscript.

Notes and references

1 BP Plc, *Bp Statistical Review of World Energy June 2015*, 64th ed.,**2015**, www.bp.com/statisticalreview
2 R. A. Dawe and S. Thomas, Energy Sources, Part A, 2007, **29**, 217-229.
3 J. H. Lunsford, *Catal. Today*, 2000, **63**, 165-174.
4 S. J. Blanksby and G. B. Ellison, *Acc. Chem. Res.*, 2003, **36**, 255-263.
5 P. Tang, Q. Zhu, Z. Wu and D. Ma, *Energ. Environ. Sci.*, 2014, **7**, 2580-2591.
6 G. Gajewski and C. W. Pao, *J. Chem. Phys.*, 2011, **135**, 064707.
7 W. Zhang, P. Wu, Z. Li and J. Yang, *J. Phys. Chem. C*, 2011, **115**, 17782-17787.
8 S. Yuan, L. Meng and J. Wang, *J. Phys. Chem. C*, 2013, **117**, 14796-14803.
9 S. Bae, H. Kim, Y. Lee, X. Xu, J. S. Park, Y. Zheng, J. Balakrishnan, T. Lei, H. Ri Kim, Y. I. Song, Y. J. Kim, K. S. Kim, B. Özyilmaz, J. H. Ahn, B. H. Hong and S. Iijima, *Nat. Nanotechnol.*, 2010, **5**, 574-578.
10 T. Kobayashi, M. Bando, N. Kimura, K. Shimizu, K. Kadono, N. Umezu, K. Miyahara, S. Hayazaki, S. Nagai, Y. Mizuguchi, Y. Murakami and D. Hobara, *App. Phys. Lett.*, 2013, **102**, 023112.
11 I. Alstrup, I. Chorkendorff and S. Ullmann, *Surf. Sci.*, 1992, **264**, 95-102.
12 B. Xing, X. Y. Pang and G. C. Wang, *J. Catal.*, 2011, **282**, 74-82.
13 B. Xing and G. C. Wang, *Phys. Chem. Chem. Phys.*, 2014, **16**, 2621-2629.
14 J. S. Yoo, T. S. Khan, F. Abild-Pedersen, J. K. Nørskov and F. Studt, *Chem. Commun.*, 2015, **51**, 2621-2624.
15 A. Soon, M. Todorova, B. Delley and C. Stampfl, *Phys. Rev. B: Condens. Matter Mater. Phys.*, 2006, **73**, 165424.
16 J. F. Weaver, *Chem. Rev.*, 2013, **113**, 4164-4215.
17 J. F. Weaver, C. Hakanoglu, A. Antony and A. Asthagiri, *Chem. Soc. Rev.*, 2014, **43**, 7536-7547.
18 A. Hellman, A. Resta, N. M. Martin, J. Gustafson, A. Trinchero, P. A. Carlsson, O. Balmes, R. Felici, R. Van Rijn, J. W. M. Frenken, J. N. Andersen, E. Lundgren and H. Grönbeck, *J. Phys. Chem. Lett.*, 2012, **3**, 678-682.
19 Y. H. Chin, C. Buda, M. Neurock and E. Iglesia, *J. Am. Chem. Soc.*, 2013, **135**, 15425-15442.
20 C.-C. Wang, S. S. Siao and J.-C. Jiang, *J. Phys. Chem. C*, 2012, **116**, 6367-6370.
21 T. L. M. Pham, E. G. Leggesse and J. C. Jiang, *Catal. Sci. Tech.*, 2015, **5**, 4064-4071.
22 Q. Zhang, K. Zhang, D. Xu, G. Yang, H. Huang, F. Nie, C. Liu and S. Yang, *Prog. Mat. Sci.*, 2014, **60**, 208-237.
23 P. N. Amaniampong, Q. T. Trinh, B. Wang, A. Borgna, Y. Yang and S. H. Mushrif, *Angew. Chem. Int. Ed.*, 2015, **54**, 8928-8933.
24 P. Hohenberg and W. Kohn, *Phys. Rev.*, 1964, **136**, B864-B871.
25 W. Kohn and L. J. Sham, *Phys. Rev.*, 1965, **140**, A1133-A1138.
26 G. Kresse and J. Furthmüller, *Phys. Rev. B: Condens. Matter Mat. Phys.*, 1996, **54**, 11169-11186.
27 G. Kresse and J. Furthmüller, *Comput. Mat. Sci.*, 1996, **6**, 15-50.
28 J. P. Perdew, K. Burke and M. Ernzerhof, *Phys. Rev. Lett.*, 1996, **77**, 3865-3868.
29 P. E. Blöchl, *Phys. Rev. B*, 1994, **50**, 17953-17979.
30 G. Kresse and D. Joubert, *Phys. Rev. B*, 1999, **59**, 1758-1775.
31 V. I. Anisimov, J. Zaanen and O. K. Andersen, *Phys. Rev. B*, 1991, **44**, 943-954.
32 M. Nolan and S. D. Elliott, *Phys. Chem. Chem. Phys.*, 2006, **8**, 5350-5358.
33 D. Wu, Q. Zhang and M. Tao, *Phys. Rev. B: Condens. Matter Mat. Phys.*, 2006, **73**, 235206.
34 V. I. Anisimov, F. Aryasetiawan and A. I. Lichtenstein, *J. Phys.: Condens. Matter*, 1997, **9**, 767-808.
35 S. L. Dudarev, G. A. Botton, S. Y. Savrasov, C. J. Humphreys and A. P. Sutton, *Phys. Rev. B: Condens. Matter Mater. Phys.*, 1998, **57**, 1505-1509.
36 Q. T. Trinh, J. Yang, J. Y. Lee and M. Saeys, *J. Catal.*, 2012, **291**, 26-35.
37 Q. T. Trinh, K. F. Tan, A. Borgna and M. Saeys, *J. Phys. Chem. C*, 2013, **117**, 1684-1691.
38 R. F. W. Bader, *Atoms in Molecules: A Quantum Theory*, Oxford University Press, USA, 1990.
39 G. Henkelman, A. Arnaldsson and H. Jónsson, *Comput. Mater. Sci.*, 2006, **36**, 354-360.
40 H. J. Monkhorst and J. D. Pack, *Phys. Rev. B*, 1976, **13**, 5188-5192.
41 S. Åsbrink and L. J. Norrby, *Acta Crystallogr., Sect. B: Struct. Sci., Cryst. Eng. Mater.*, 1970, **26**, 8-15.
42 J. Hu, D. Li, J. G. Lu and R. Wu, *J. Phys. Chem. C*, 2010, **114**, 17120-17126.
43 X. Jiang, T. Herricks and Y. Xia, *Nano Lett.*, 2002, **2**, 1333-1338.
44 F. Bayansal, S. Kahraman, G. Ankaya, H. A. Etinkara, H. S. Güder and H. M. Akmak, *J. Alloys Comp.*, 2011, **509**, 2094-2098.
45 R. Bari, S. Patil and A. Bari, *Int. Nano Lett.,* 2013, **3**, 1-5.
46 C. Stampfl, A. Soon, S. Piccinin, H. Shi and H. Zhang, *J. Phys.: Condens. Matter*, 2008, **20**, 184021.

View Article Online
DOI: 10.1039/C5CY01784J

47 K. Zhou, R. Wang, B. Xu and Y. Li, *Nanotechnology*, 2006, **17**, 3939-3943.
48 Y. Li, B. Tan and Y. Wu, *Chem. Mat.*, 2008, **20**, 567-576.
49 B. Ruscic, J. E. Boggs, A. Burcat, A. G. Császár, J. Demaison, R. Janoschek, J. M. L. Martin, M. L. Morton, M. J. Rossi, J. F. Stanton, P. G. Szalay, P. R. Westmoreland, F. Zabel and T. Bérces, *J. Phys. Chem. Ref. Data*, 2005, **34**, 573-588.
50 J. H. Lunsford, *Angew. Chem. Int. Ed. Eng.*, 1995, **34**, 970-980.
51 Y. H. Chin, C. Buda, M. Neurock and E. Iglesia, *J. Am. Chem. Soc.*, 2011, **133**, 15958-15978.
52 K. Tanabe and T. Yamaguchi, *Catal. Today*, 1994, **20**, 185-197.
53 S. Adhikari, A. Üren and R. Roy, *J. Biol. Chem.*, 2008, **283**, 1334-1339.
54 W. J. Van Zeist and F. M. Bickelhaupt, *Org. Biomol. Chem.*, 2010, **8**, 3118-3127.
55 I. Fernández and F. M. Bickelhaupt, *Chem. Soc. Rev.*, 2014, **43**, 4953-4967.
56 A. Vojvodic, F. Calle-Vallejo, W. Guo, S. Wang, A. Toftelund, F. Studt, J. I. Martínez, J. Shen, I. C. Man, J. Rossmeisl, T. Bligaard, J. K. Nørskov and F. Abild-Pedersen, *J. Chem. Phys.*, 2011, **134**, 244509.
57 J. K. Nørskov, T. Bligaard, A. Logadottir, S. Bahn, L. B. Hansen, M. Bollinger, H. Bengaard, B. Hammer, Z. Sljivancanin, M. Mavrikakis, Y. Xu, S. Dahl and C. J. H. Jacobsen, *J. Catal.*, 2002, **209**, 275-278.
58 A. Michaelides, Z. P. Liu, C. J. Zhang, A. Alavi, D. A. King and P. Hu, *J. Am. Chem. Soc.*, 2003, **125**, 3704-3705.
59 R. A. Van Santen, I. Tranca and E. J. M. Hensen, *Catal. Today*, 2015, **244**, 63-84.
60 P. V. Madhavan and M. D. Newton, *J. Chem. Phys.*, 1985, **83**, 2337-2347.
61 J. Zhang, Z. Wang, T. Niu, S. Wang, Z. Li and W. Chen, *Sci. Rep.*, 2014, **4**, 4431.
62 J. J. Varghese and S. H. Mushrif, *J. Chem. Phys.*, 2015, **142**, 184308.
63 Y. Shibuta, R. Arifin, K. Shimamura, T. Oguri, F. Shimojo and S. Yamaguchi, *Chem. Phys. Lett.*, 2014, **610-611**, 33-38.
64 J. S. Lee and S. T. Oyama, *Catal. Rev.*, 1988, **30**, 249-280.
65 X. Guo, G. Fang, G. Li, H. Ma, H. Fan, L. Yu, C. Ma, X. Wu, D. Deng, M. Wei, D. Tan, R. Si, S. Zhang, J. Li, L. Sun, Z. Tang, X. Pan and X. Bao, *Science*, 2014, **344**, 616-619.
66 S. Grundner, M. A. C. Markovits, G. Li, M. Tromp, E. A. Pidko, E. J. M. Hensen, A. Jentys, M. Sanchez-Sanchez and J. A. Lercher, *Nat. Commun.*, 2015, **6**, 7546

View Article Online
DOI: 10.1039/C5CY01784J

Table of Contents: Graphical Abstract

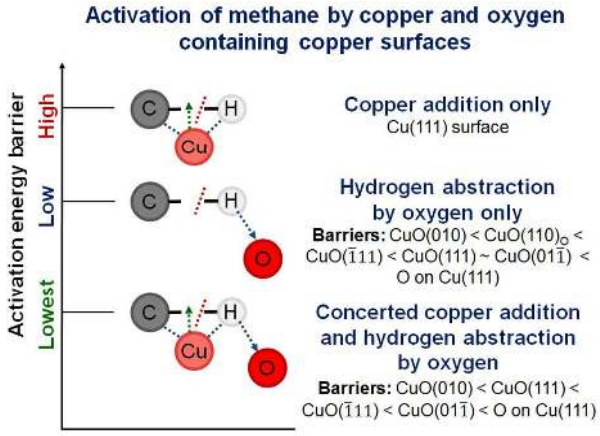

Abstract: Of the three mechanisms for activation of methane on copper and copper oxide surfaces, the under-coordinated Cu-O site pair mediated mechanism on CuO surfaces has the lowest activation energy barriers.